YU ISSN 0015—3206
FZKAAA 15 (4) 331 (1983)

IN SITU ELECTRICAL AND OPTICAL OBSERVATION OF Ti THIN FILM OXIDATION

STJEPAN LUGOMER and MLADEN STIPANČIĆ

Electrotechnical faculty, 78000 Banja Luka, Yugoslavia

Received 12 April 1983

UDC 538.975

Original scientific paper

High temperature Ti thin film oxidation was studied in the intermediate interval between logarithmic and parabolic oxidation kinetics. A gradual increase of the logarithmic oxidation rate, instead of the expected gradual transition from logarithmic to parabolic kinetics, was observed. The contribution of the parabolic oxidation kinetics was found to be constant, and insensitive to the thermal treatment. The study was done on the basis of simultaneous »IN SITU« electric resistivity and multiple beam interferometry (*MBI*) reflection measurements. Transmission microscopy (*TEM*) and Auger Electron Spectroscopy (*AES*) depth profiles studies have shown that the homogenous TiO_2 rutile structure was invariant to the kinetics variation. *MBI* reflection curves, fitted on the basis of the model of semitransparent film predicted amplitude convergence to the bulk reflection value and phase divergence with increasing film thickness. Amplitude fitting better than 85% and phase fitting better than 95% were obtained. The extinction coefficient β for TiO_2 rutile, at $\lambda = 632.8$ nm (He-Ne laser), was found to be $3.6 \cdot 10^4\ cm^{-1}$.

1. Introduction

The oxidation of thin Ti films was studied by a number of authors (see P. Kofstad[1]) and references cited therein). However, the variation of electrical resistivity R_Ω, reflectivity R, and transmitivity T, as a function of the oxidation time τ, seems not to have been investigated so far.

We investigated the oxidation kinetics by *in situ* resistivity and multiple beam interferometry (*MBI*) reflectivity measurements. In particular, we paid attention to the intermediate interval of oxidation temperatures ~ 700 K still not well

elucidated, which is characterised by two simultaneous oxidation kinetics: a logarithmic one and a parabolic[1] one.

Our starting assumption was that the samples held at 750 K would be oxidized by almost purely parabolic kinetics, while those oxidized at lower temperatures or at temperature continually increasing from 300 K to 700 K by various heating rates, would be oxidized by various degree of logarithmic and parabolic kinetics[1].

By increasing the heating rates, participation of the parabolic with respect to the logarithmic oxidation rate was expected to increase. *In situ* electric measurements enable us to follow the initial phase (I), the intermediate phase (II) and the final oxidation phase (III), respectively, and to determine the dominant rate dependent conductivity mechanism in every particular phase. While the conductivity mechanisms are the subject of a separate paper[2], in this paper we concentrated on the discussion of oxidation kinetics by fitting the curves $d = f(\tau)$ with the combined logarithmic-parabolic equation and on the determination of the oxidation delay.

Simultaneous *in situ MBI* reflection measurements were undertaken to investigate the optical properties of Ti-oxide films, as well as to verify the Browell--Anderson model[3]. Application of this model to the Ti-oxide semitransparent film predicts convergence of $R_{max} - R_{min}$, and a divergence of the phase. On this basis the extinction coefficient of TiO_2 thin film can be determined.

Prior to the optical and electrical measurements analysis, it is necessary to know the Ti-oxide structure. From this point of view it was of interest to investigate whether the different oxidation rates influenced the homogeneity and eventually the crystallographic structure of Ti-oxide films.

For this reason transmission electron microscopy (*TEM*), structural studies and Auger Electron Spectroscopy (*AES*) depth profiling were performed and compared with the existing results of Hurlen[4], Guenther and Pulker[5], and Mathieu and Landolt[6].

2. *Experimental*

The experimental procedure comprised two successive steps:

1. Ti films were evaporated by means of an electron gun onto a quartz substrate in a *VARIAN NRC* 836 evaporator. The pressure was held at $133.3 \cdot 10^{-6}$ Pa, while the film thickness was controlled with a *VARIAN ADS* 200 automatic programer/controller. The purity of Ti was 99.95%, and the deposition rate of 2 nm/s was used.

2. The obtained Ti films were oxidized in two ways — either at the constant temperature of 700 K, with parabolic kinetics[1] (group I), or by increasing the temperature from 420 K to 700 K, with the oxidation being initially logarithmic and changig into the parabolic one as the temperature increased (group II).

The structure of the as evaporated and oxidized films was investigated by means of transmission electron microscopy (*TEM*) in a *PHILIPS EM* 301. The samples were prepared by stripping the films off the substrate in a *HF* vapor and by mounting the washed films onto 400-*MESH* microscope grids.

Concentration profiles from the Ti/O ratios were determined by *AES* depth profiling Ti *LMM* (418 eV) ond O *KLL* (510 eV). Oxide layers were etched off by Ar^+ ion bombardment with a rate of 1 nm/min. Multiple beam interference (*MBI*) reflection has been investigated with an experimental set-up, similar to the one described by Ruiz-Urbieta et al.[7]. Since the interferometric change is directly related to the oxidation kinetics, *MBI* is an ideal method for the *in situ* experiments. Its oscillation period depends on the incidence angle, the real index of refraction, the light wavelength and the oxidation rate. For a given wavelength, and a known oscillation period, the oxidation rate, the refraction index and the extinction coefficient can be determined.

3. Results and discussion

The structure: *TEM* studies were performed on films of both groups, I and II. It was found that, regardless of the oxidation kinetics, oxidized films have a uniform, small grain morphology, shown in Fig. 1a. It was found from the corresponding diffraction pattern (Fig. 1b), that only pure rutile TiO_2 grains form the thin films. The measured interplanar distances, as well as those corresponding to rutile according to *ASTM* no. 21—1276 are given in Table 1.

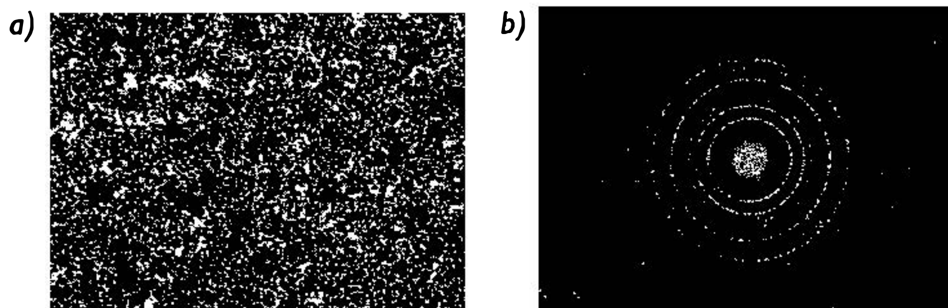

Fig. 1. a) The micrograph of a typical rutile TiO_2 thin film. (Magnification 70 000 X), and b) the corresponding diffraction pattern.

TABLE 1

d_{exp}/nm	d_{TiO_2}/nm	khl_{TiO_2}
0.323	0.325	110
0.246	0.2487	101
0.228	0.2297	200
0.216	0.2188	111
0.204	0.2051	210
0.167	0.1687	211

The same structure was obtained for both group of samples, i. e. for both oxidation kinetics.

AES depth profiles

The depth dependent concentration of Ti and O was determined from the *AES* depth profiles fo Ti *LMM* (418 eV) and O *KLL* (510 eV) peaks, as functions of the etching time. Beam current density was 0.5 μA/cm^2, *RC* was 0.1 s and modulation voltage was 6 V.

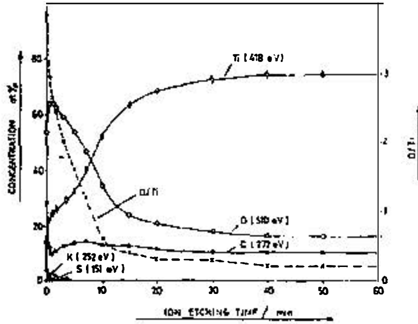

Fig. 2. The *AES* depth profiles of as evaporated Ti thin film exposed to air (E = 3 KeV, V_{MOD} = 6 V, RC = 0.1 s; Ion etching rate = 1 nm/min).

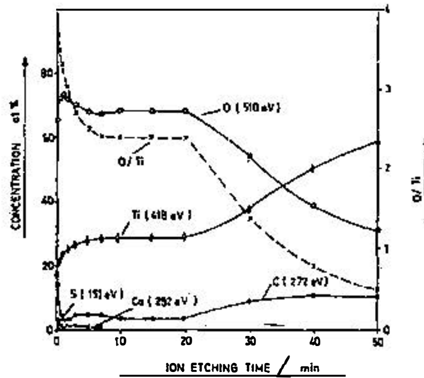

Fig. 3. The *AES* depth profiles of partially oxidized Ti thin film.

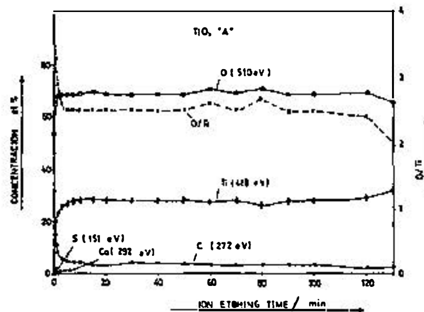

Fig. 4. The *AES* depth profiles of completely oxidized Ti thin film (Group I and II).

The depth profiles are given in Figs. 2—4, of which Figs. 2 and 3 are related to the gradual oxidation of Ti, while Fig. 4 is related to the completely oxidized Ti film. Note the high oxigen concentration at the surface (adsorbed oxigen) of the as evaporated Ti film after exposed to the air (Fig. 2). This implies the presence of multiple oxidation, the first step of which begins by exposure of the as evaporated films to air, and the second by submission on these films to oxidation treatment. This problem was well elaborated in the article by Deal and Grove[8] for the thermal oxidation of Si, and observed in the references cited therein.

The oxide skin has a thickness of less than 10 nm and prevents oxygen penetration from the surface and thus blocks the oxidation. When Ti film is exposed to increased temperature, oxidation proceeds after a time (delay) τ_0, which will be determined by electric measurements. In this case, again a high oxygen concentration was found at the surface (Fig. 3), which decreases to $\sim$ 5nm below the surface, after which it stays constant throughout the film.

Similar characteristics were found in completely oxidized films of groups I and II. (Fig. 4). Impurities like S, C and Cl were always present and these seem to be present in Ti-oxides even when very pure material and more rigorous vacuum conditions were used[9]. The C-peak changes from a shape typical for adsorbed carbon, to the one characteristic for TiC. In general, our *AES* depth profiling results are similar to the ones of Mathieu and Landolt[6], and they show that oxidation was homogenous in all cases regardless of thermal treatment, and therefore invariant to the oxidation kinetics.

Electric resistivity

In situ resistivity measurements (Fig. 5) were used for the determination of oxidation time delay τ_0, as well as for the determination of the oxidation rate. Conductivity mechanisms are only mentioned; their analysis and detailed discussion will be given in a separate paper [2]. From Fig. 5 there typical oxidation phase could clearly be distinguished:

Phase I — the initial phase, with $R_\Omega = 180\,\Omega$; that means that the oxidation did not start at $\tau = 0$. It started after a time delay τ_0 which is rate dependent. According to Fig. 5, $\tau_0 = 30$ min for curve c, 50 min for curve b and 90 min for curve a represent the time necessary to reach the activation temperature for ion diffusion and the time for oxygen to be transported from the surface through the oxide layer. It has to be mentioned that the oxide layer which is < 10 nm thick, as can be seen from the *AES* depth profiles in Fig. 2 (i. e. between 30 and 40 atomic distances according to Table 1 for TiO_2 rutile), can grow to some extent without influencing the conductivity at a measurable level. This rather general problem of the actual beginning of oxidation is particularly important when an oxide grows very slowly in one temperature interval and very fast in an other, as was the case in our experiments, and as Wagner and Wilmsen reported for the case of thermal oxidation of InP[10].

For the same reason R_Ω (Fig. 5) is constant, insensitive to the oxidation kinetics, and the same for both group (I and II) of samples. The conductivity is predominantly of a metallic nature.

Phase II. The resistance interval $R_\Omega = 200\,\Omega$ to $10\,k\Omega$ corresponds to the period of intensive oxidation, which is characterised by the contribution of two conductivity terms:

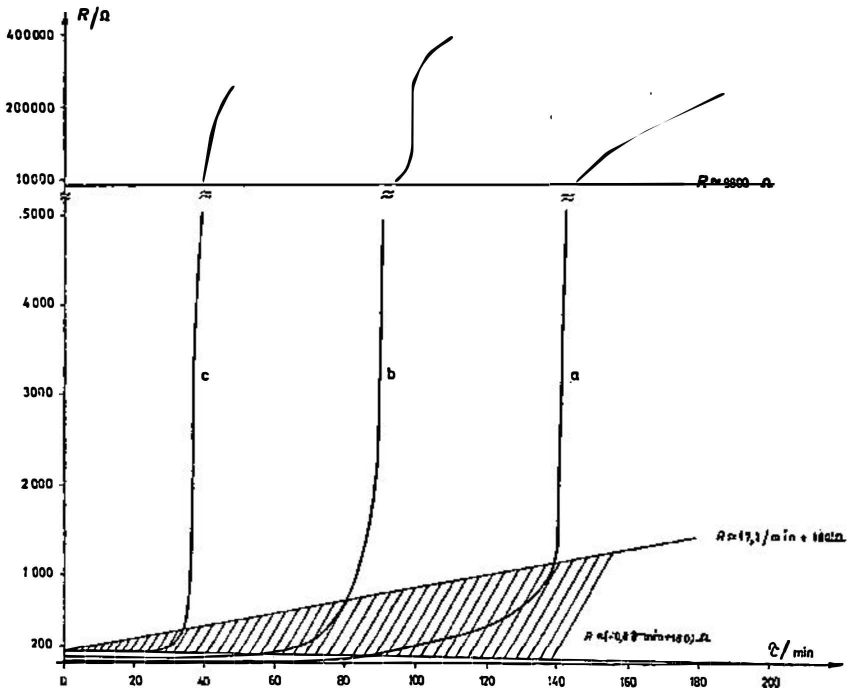

Fig. 5. Electric resistivity as the function of oxidation time. Curves b and c belong to group II, and curve a, to group I, of the samples.

(i) the conductivity of metallic Ti thin film, which decreases with τ.

(ii) The n-tipe conductivity of TiO_2 which increases with τ. In this phase R_Ω is a linear function of the oxidation time

$$R_{\Omega II} = \text{const.}\ \tau,$$

regardless of the oxidation treatment. A rough estimate from curves a, b, and c in Fig. 5 gives:

$R_{\Omega II abc} \cong 800\ \tau\ \Omega/\text{min} \simeq C$ where C depends on a, b and c.

This is a significant relation, because the linear coefficient $\Delta R_\Omega / \Delta \tau$ is the same for all treatments. Curves $R_\Omega(\tau)$ in Fig. 5 are almost parallel straight lines, which means that the conductivity mechanism is not sensitive to the oxidation kinetics. It also means that the oxigen diffusion mechanism is more affected by inherent structural properties of the Ti-film that by external conditions, like thermal treatment.

Phase III. The final oxidation phase with $R_\Omega > 10\ \text{k}\Omega$. This period is characterised by the domination of the n-type conductivity of TiO_2. The shape of the curve $R_\Omega = f(\tau)$ is expected to be determined by scattering charge carriers on

impurities and structural defects, so that the electrical resistivity is proportional to τ^n:

$$R_{\Omega} \sim \tau^n \quad n < 1,$$

where the exponent n depends on oxidation kinetics. For this reason it is different for the curve a, b and c in Fig. 5.

Oxidation phases I and II are bridged by a transition interval characterised by the bent part of the curve $R_{\Omega} = f(\tau)$. It lies between:

$$\tau = 30 \text{ min to } \tau = 40 \text{ min for curve c,}$$

$$\tau = 50 \text{ min to } \tau = 90 \text{ min for curve b and}$$

$$\tau = 90 \text{ min to } \tau = 150 \text{ min for curve a.}$$

The width of this interval is inversely proportional to the oxidation rate and defined by two straight lines:

$$R_{\Omega} = (-0.7\ \tau/\text{min} + 180)\ \Omega$$

$$R_{\Omega} \simeq (-0.8\ \tau/\text{min} + 180)\ \Omega$$

represented by the shadowed area in Fig. 5. It means that all $R = f(\tau)$ curves, regardless of the oxidation kinetics, belong to the same family.

The width of the transition interval is inversely proportional to the oxidation rate. This interval depends heavily on oxidation kinetics; it moves to the left and to the right (in Fig. 5) for higher and lower oxidation rates, respectively.

Oxidation kinetics curves $d = f(\tau)$ (Fig. 6) were obtained from the curves in Fig. 5, taking into account that R_{Ω} depends on the film dimensions, and supposing that all dimensions were constant during oxidation, except thickness.

We have also taken into account that electric resistivity ϱ, was constant with the film thickness d. As can be seen from the literature, this is the case for:

Ag film: ϱ = const. for $d > 50$ nm[11]

Rh film: ϱ = const. for $d > 55$ nm[12]

Nb film: ϱ = const. for $d > 50$ nm[13]

Al film: ϱ = const. for $d > 100$ nm[14].

In the case of Ti oxidation of the starting thickness of 200 nm, ϱ = constant, until the remaining unoxidized Ti-film thickness stays above 50 nm. The unoxidized film thickness can be obtained from the difference of the starting film thickness and the oxide thickness divided by the Piling-Bedworth factor $a = 1.64$ for TiO_2 and according to Fig. 6, the above condition was fulfilled.

Following our starting assumption the oxidation reaction may be described by a logarithmic rate equation, due to the electric field induced transport of ions through the film, during initial stages at low temperatures. The rate of reaction

by this mechanism will eventually become slower than the rate of reaction due to thermal diffusion of the ions. The oxidation can be described by a combination of the logarithmic and parabolic rate equations[1]:

$$d = K_e \ln(\tau + t) + K_p \tau^{1/2} + C, \tag{1}$$

where t is adjusting parameter, K_e and K_p are the logarithmic and parabolic rate constants, respectively. The interval of validity of this combined equation has to be established in every particular case. Fitting of the curves a, b and c with this equation is presented in Fig. 6.

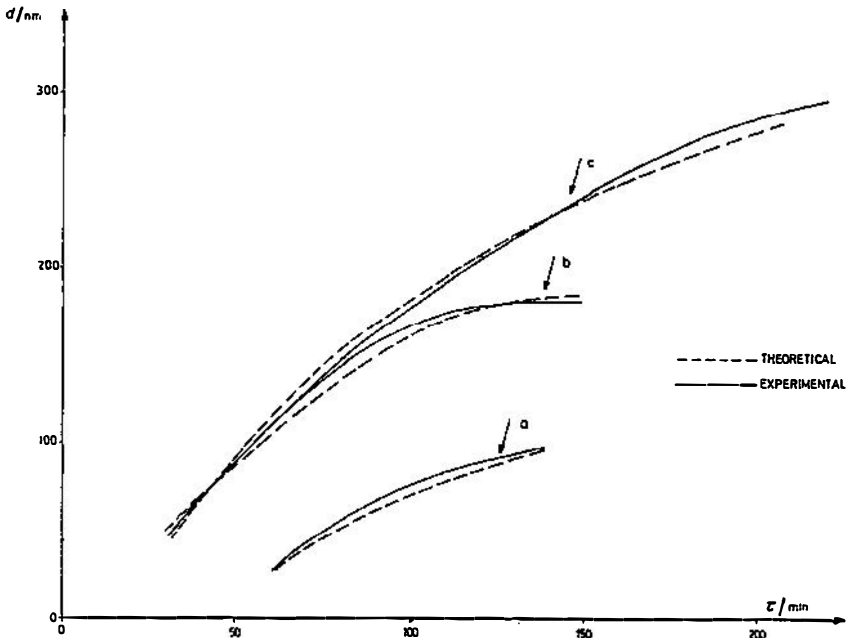

Fig. 6. The oxidation kinetics curves $d = f(\tau)$. Curves a, b and c relate to groups II and I, respectively, as given in Fig. 5.

The logarithmic and parabolic rate constants, as well as t and C, are given in Table 2.

A very good fitting of the oxidation curves a, b and c, was obtained in the following time intervals:

curve a: between 60 min and 140 min,

curve b: between 30 min and 140 min,

curve c: between 30 min and 210 min.

TABLE 2

	K_e	K_p	t	C
a	85	10	5	−312
b	60	10	5	−220
c	40	10	5	−215

It follows from Table 2, that logarithmic oxidation kinetics increases by passing from the curve a, to b to c, while the parabolic stays constant and insensitive to the thermal treatment. This means that we did not observe a gradual transition from the logarithmic oxidation kinetics to the parabolic one, but only a gradual increase of the logarithmic oxidation rate. This result differs from our starting assumption, and from the suggestion in the literature[1]. In our opinion the literature statement is valid for somewhat higher temperatures.

This also means that in the intermediate interval we observed a gradual increase of the electric field induced diffusion belonging to the logarithmic oxidation rate, instead of a gradual transition to the thermally induced diffusion belonging to the parabolic one. The explanation may well be that the gradual temperature increase resulted in increased dissociation of O_2 molecules in the gas-oxide interface, and the increased chemisorption of oxygen atoms[15]. Therefore, the surface potential in the oxide layer (caused by chemisorption of O atoms with negative polarization) increased, which made field induced diffusion increase with the temperature. However, it has to be mentioned that the mechanisms of Ti oxidation are still not well established. Because our structural studies have shown a small-grain morphology of TiO_2, meaning that grain-boundary area covers a great deal of the total area, we believe that grain boundary diffusion may be an additional oxygen diffusion mechanism besides the two previously mentioned. It may well be that this mechanism, as a very efficient oxygen transport mechanism, is responsible for TiO_2 formation as the highest oxide of titanium.

MBI reflection

Variation of oxidation kinetics did not show any influence on the structure of Ti-oxide.

Henceforth basic optical parameters like real and imaginary refraction index, absorption coefficient etc. are constant and rate independent. However, light reflected from the interface film/air, interferes with light reflected from the interface oxide/metal, and a resulting signal from a photodetector oscillates depending on whether the thickness of the oxide film satisfies conditions for interference maxima or minima. As the oxide thickness grows in time, the reflection which depends on thickness becomes rate dependent. For this reason the *MBI* reflection study can give information about oxidation kinetics. As the kinetics was discussed on the basis of electric measurements, attention will be paid to:

(i) verification of existing theoretical models for *MBI* reflection, and

(ii) determination of the extinction coefficient of the TiO_2 rutile.

One representative curve of *MBI* reflection $R = f(\tau)$ was chosen, and after determination of the $d = f(\tau)$ dependence it was transformed in $R = f(d)$, which is represented by the broken curve in Figs. 7a, b, c.

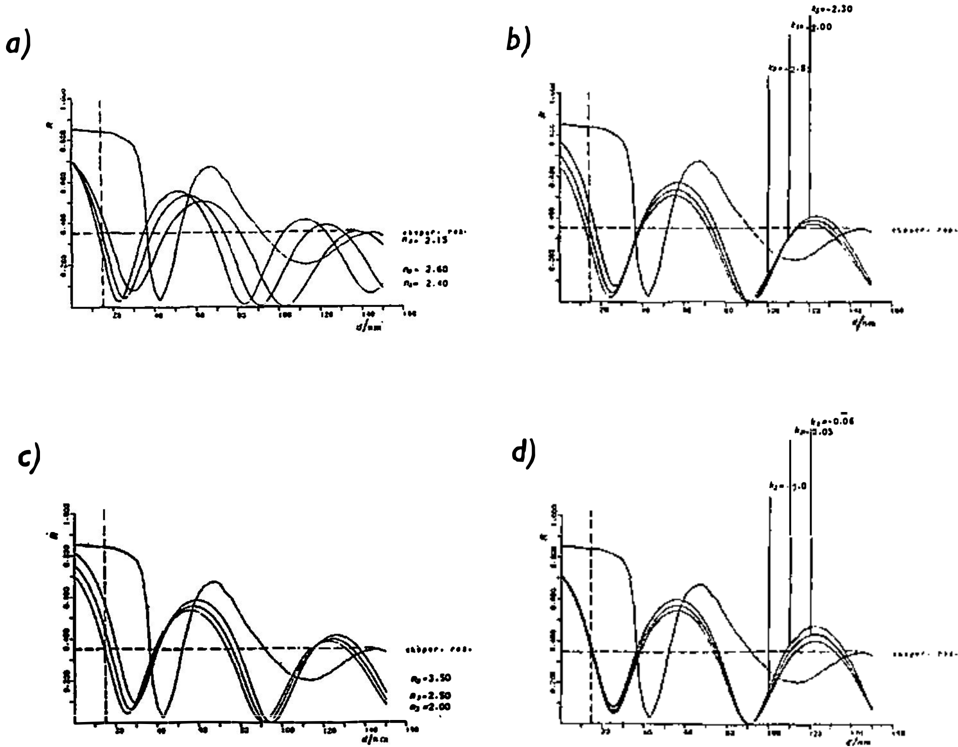

7. Fitting of the *MBI* reflection curves. Variable parameters n_2, k_2, n_3, k_3, for curves a, b, c and d, respectively.

Interpretation of *MBI* reflection results requires application of the appropriate theoretical model, previously verified. The widely used model for transparent films[16,17] does not give satisfactory result with respect to the experimentally established:

(i) amplitude convergence to the bulk reflection value, and

(ii) phase divergence.

For this reason a more complex model for a semitransparent or slightly absorbing film has to be taken into account. Starting with this supposition in mind, we find out the calculation which Ruiz-Urbieta[7] applied in the case of aluminium oxide film on pure aluminium and a zirconium oxide film on pure aluminium, and the calculation of Browell-Anderson for the ice of ($NH_3 + H_2O$) film on a substrate of saphire[3], can be applied in our case. Taking into account the *normal geometry* of the experiment i. e. laser beam vertical to the film surface, reflection

R, of a monochromatic, perpendicularly polarised light which strikes the absorbing Ti- oxide film, deposited onto an absorbing substrate is given[3]:

$$R = \frac{\varrho_{12}^2 + \varrho_{23}^2 e^{4v_2\eta} + 2\,\varrho_{12}\,\varrho_{23}\,e^{-2v_2\eta}\cos(\varphi_{23} + 2u_2^\eta)}{1 + \varrho_{12}^2\,\varrho_{23}^2\,e^{4v_2\eta} + 2\varrho_{12}\,\varrho_{23}\,e^{-2u_2\eta}\cos(\varphi_{23} + 2\,u_2^\eta)}\,. \tag{2}$$

where the indices 1, 2, 3, 12 and 23 are related to air above the film, the film, the substrate, the air/oxide interface and the oxide/substrate interface. ϱ_{12} and ϱ_{23} in (2) are reflection coefficients of interfaces, and φ_{12} and φ_{23} are corresponding phase changing on interfaces. The film thickness, d, is substituted by dimensionless thickness η defined as:

$$\eta = \frac{2\pi\, d}{\lambda_0}, \tag{3}$$

where λ_0 is the light wavelegth in the vacuum, ϱ_{12}, ϱ_{23}, φ_{12} and φ_{23} are defined in terms of incidence angle ϑ, indexes of refraction of the air n_1, film $n_2\,(1 + ik_2)$ and substrate $n_3\,(1 + ik_3)$:

$$\varrho_{12}^2 = \frac{(n_1\cos\vartheta_1 - u_2)^2 + v_2^2}{(n_1\cos\vartheta_1 + u_2^2) + v_2^2},$$

$$\varrho_{23}^2 = \frac{(u_2 - u_3)^2 + (v_2 - v_3)^2}{(u_2 + u_3)^2 + (v_2 + v_3)^2}, \tag{4}$$

$$\varphi_{12} = \mathrm{tg}^{-1}\left|\frac{2v_2\, n_1\cos\vartheta_1}{u_3^2 + v_2^2 - n_1^2\cos\vartheta_1}\right| \tag{5}$$

$$\varphi_{23} = \mathrm{tg}^{-1}\left|\frac{2\,(u_3\, v_2 - u_2\, v_3)}{u_2^2 - u_3^2 + v_2^2 - v_3^2}\right|. \tag{6}$$

Constants are defined as follows:

$$2u_2^2 = c + (c^2 + d)^{1/2}, \quad 2\,v_2^2 = -\,c + (c^2 + d)^{1/2},$$

where

$$c = n_2^2\,(1 - k_2^2) - n_1^2\sin^2\vartheta_1, \quad d = 4n_2^4\,k_2^2,$$

$$2\,u_3^2 = a + (a^2 + b)^{1/2}, \quad 2\,v_3^2 = -\,a + (a^2 + b)^{1/2} \tag{7}$$

with

$$a = n_3^2\,(1 - k_3^2) - n_1^2\sin^2\vartheta_1, \quad b = 4\,n_3^4\,k_3^2. \tag{8}$$

Pulker, Presold and Ritter[18] have found for Ti-oxide series the n_2 values as a function of oxigen pressure (PO_2), substrate temperature and deposition rate.

They found that n_2 varies between 2.21 and 2.62 for TiO, and between 2.10 and 2.41 for TiO_5. For oxide like TiO_2 and the nonstoichiometric TiO_x ($x < 1$) there are no data, but it can be supposed that n_2 for TiO_2 lies in the same interval. We found no data in the literature for k_2, but calculation and fitting of experimental curves $R = f(d)$ have shown that $n_2 k_2 \sim 0.1$. Following the Browell-Anderson type of calculation of R, we shall suppose that the refraction index n_2 is higher than 1. Actually, for TiO_2, $n_2 > 2$. In this case, one finds:

$$3 n_2 k_2 \ll 1, \quad 3 k_2^2 \ll 1, \quad k_2^4 \ll 1.$$

With these approximations, it follows from (7):

$$v_2^2 = \frac{n_2^4 k_2^2}{n_2^2 - n_1^2 \sin^2 \vartheta_1} \tag{8a}$$

$$u_2^2 = n_2^2 - n_1^2 \sin^2 \vartheta_1. \tag{8b}$$

Reflection extrema are given by:

$$R_{ext} = \frac{\varrho_{12}^2 + \varrho_{23}^2 e^{-2\beta h} \pm 2 \varrho_{12} \varrho_{23} e^{-\beta h}}{1 + \varrho_{12}^2 \varrho_{23}^2 e^{-2\beta h} \pm 2 \varrho_{12} \varrho_{23} e^{-\beta h}} \tag{9}$$

where ... (+) relates to R_{max} and ... (−) to R_{min}.

A further condition is that ϱ_{12} and ϱ_{23} are positive and that $0 < \varphi_{23} < \pi$. The exponent in (9) is the extinction coefficient, derived from $R_{max} - R_{min}$:

$$R_{max} - R_{min} = \frac{4 \varrho_{12} \varrho_{23} e^{-\beta h} (1 - \varrho_{12} \varrho_{23} e^{-2\beta h})}{1 - 4 \varrho_{12}^2 \varrho_{23}^2 e^{-2\beta h}}. \tag{10}$$

Numerical calculations of R on the basis of this model and experimental curves $R = f(d)$ for TiO_2, are given as parametric functions of n_2, k_2 in Fig. 7a and Fig. 7b, and as functions of n_3, k_3 in Fig. 7c and Fig 7d.

The parameters used are as follows:

Fig. 7a. n_2 ($n_2 = 2.40$; 2.60)

Fig. 7b. k_2 ($k_2 = -0.05$; -0.06; -0.07)

Fig. 7c. n_3 ($n_3 = 2$; 2.5; 3.5)

Fig. 7d. k_3 ($k_3 = -2$; 2.3; -2.8)

and D is half of the film thickness ($D = d/2$). The best fitting with respect to the amplitude and phase is obtained in Fig. 7.

The extinction of ($R_{max} - R_{min}$), characterised according to Browell-Anderson by the extinction coefficient β, is:

$$\beta = \frac{1}{d_2 - d_1} \ln \left[\frac{(R_{max} - R_{min}) / d_1}{(R_{max} - R_{min}) / d_2} \right]. \tag{11}$$

Since the reflection is proportional to the signal detector, S, this relation can be written as:

$$\beta = \frac{1}{d_2 - d_1} \ln \left[\frac{(S_{max} - S_{min}) / d_1}{(S_{max} - S_{min}) / d_2} \right], \tag{12}$$

which gives for a He-Ne laser ($\eta = 2\,637.1\, n$) for TiO_2, a value of: $\beta = 3.6 \cdot 10^4\ cm^{-1}$. To our knowledge this is the first determination of the extinction coefficient of TiO_2. It is 2—3 times lower than for the Ta-oxide[19].

Amplitude ($R_{max} - R_{min}$) $= f(d)$ converges to the bulk reflection value R_{bulk}, (horizontal dashed line in Figs. 7a to c), while phase diverges with increased d as Shanley et al., have shown in the case of CuO[20]. The overall behaviour of the reflection curves $R = f(d)$, predicted by the above model, agrees completely with the phase and amplitude behaviour of the experimental curves.

The amplitude fitting is better then 75% in all cases, the phase fitting, however, requires additional discussions. The film thickness was determined by the independent electrical measurements during oxidation. However, the change of electrical resistance was higher than expected at the beginning of oxidation: Basseches[21] has shown that grain boundary oxidation caused the increase of resistance during the initial oxidation (and formation of the oxide layer), which Maissel[22] later verified. He has shown that Ta-oxide thickness obtained from electrical measurements, was for 15 nm higher than the actual thickness.

This is in agreement with *MBI* reflection measurements showing that the initial oxide reflection decreases, from the moment when oxide film reaches the thickness of 15 nm. This is what we really observed, as shown in Fig. 7. For this reason the experimental *MBI* curve in Fig. 7 has to be shifted to the left for 15 nm with respect to the theoretical curves (vertical dashed line). Taking into account this corrections our phase fitting is almost 100%.

4. *Conclusion*

The intermediate interval of Ti oxidation, between logarithmic and parabolic oxidation has not been investigated very intensively so far. By our *in situ* electric resistivity and *MBI* reflectivity measurements, we attemped to elucidate the oxidation process itself in this interval, and to establish some optical properties of TiO_2 thin film.

1. It was shown that the formation of the homogenous TiO_2 rutile structure during oxidation in the intermediate interval was invariant to the oxidation kinetics.

2. Excellent fitting of the oxidation curves, $d = f(\tau)$, on the basis of the combined logarithmic-parabolic equation, has shown a gradual increase of the logarithmic kinetics instead of the expected gradual transition from logarithmic to parabolic kinetics.

3. The interpretation of the *MBI* reflection curves, $R = f(d)$, on the basis of the model for semitransparent film and Browell-Anderson type calculation, results in amplitude fitting better than 85%, and phase fitting better than 95%, respectively. The extinction coefficient of the TiO_2 rutile and the He-Ne laser · wavelength have been determined to be $\beta = 3.6 \cdot 10^{-4}\ cm^{-1}$.

A further step in the elucidation of oxidation in the intermediate interval will be possible after completion of an electric conductivity analysis which is now in progress.

Acknowledgments

The authors wish to thank Dr. A. Prodan from the *Josef Stefan Institute*; Dr. A. Bjeliš from the *Institute of Physics*, Zagreb; Dr A. Zalar from the *Institute of Electronics and Vacuum Techniques* for *AES* depth profiling; and Mr. G. Štrkić for computational work.

References

1) Per Kofstad, *High Temperature Oxidation of Metals*, J. Willey Sons, Inc., New York, 1963;
2) S. Lugomer, M. Stipančić and M. Kerenović (in preparation);
3) E. V. Browell and R. C. Anderson, J. Opt. Soc. Am. **65** (1975) 919;
4) T. Hurlen, J. Inst. Metals **89** (1960/61) 128;
5) K. H. Guenther and H. K. Pulker, Appl. Opt. **15** (1976) 2992;
6) H. J. Mathieu and D. Landolt, Proc. 7th Intern. Vac. Congr. and 3rd Intern. Conf. Solid Surfaces, Viena, 1977;
7) M. Ruiz-Urbieta, E. M. Sparrow and E. R. G. Eckert, J. Opt. Soc. Am. **61** (1970) 351;
8) B. E. Deal and A. S. Grove, J. Appl. Phys. **36** (1965) 3707;
9) W. E. Wall, M. W. Ribarsky and J. R. Stevenson, J. Appl. Phys. **51** (1980) 661;
10) J. F. Wagner and C. W. Wilmsen, J. Appl. Phys. **51** (1980) 812;
11) I. Komnik, *Fizika metaličeskih plenok*, Moskva 1979;
12) I. Koshy, J. Phys. D: Appl. Phys. **13** (1980) 1339;
13) J. J. Cuomo, R. J. Gambino and R. Rosenberg, J. Vac. Sci. Technol. **11** (1974) 34;
14) S. K. Bandyopadhyay and A. K. Pal, J. Phys. D: Appl. Phys. **12** (1979) 953;
15 M. W. Roberts and C. S. Mc Kee, *Chemistry of the Interface Metal-Gas*, Oxford Univ. Press, 1978;
16) M. Born and E. Wolf, *Principles of Optics*, Pergamon Press, New York, 1964;
17) O. S. Heavens, *Optical Properties of Thin Solid Films*, Dover, New York, 1965;
18) H. K. Pulker, G. Presold and E. Ritter, Appl. Opt. **15** (1976) 2986;
19) S. Lugomer and M. Stipančić (in preparation);
20) C. V. Shanley, R. E. Hummel and E. D. Verink, Corosion. Sci. **20** (1970) 467.
21) H. Basseches, IRV Trans. Component Parts **CP-8** (1961) 51;
22) L. I. Maissel, in Proceedings 9th National Vac. Symp. (1962) p. 169.

IN SITU ELEKTRIČKA I OPTIČKA OPSERVACIJA OKSIDACIJE TANKOG FILMA Ti

STJEPAN LUGOMER i MLADEN STIPANČIĆ

Elektrotehnički fakultet, 78000 Banja Luka

UDK 538.975

Originalni znanstveni rad

Istraživana je visokotemperaturna oksidacija tankih filmova Ti u intermedijarnom intervalu između logaritamske i paraboličke kinetike oksidacije. Primjećeno je postepeno povećanje logaritamske kinetike umjesto očekivanog postepenog prijelaza s logaritamske na paraboličku kinetiku oksidacije. Primjećeno je također, da je parabolička kinetika neosjetljiva na termičko tretiranje. Istraživanje se temelji na simultanim *in situ* mjerenjima električnog otpora i *MBI* refleksije. Strukturne studije pomoću transmisionog elektronskog mikroskopa i Augerovog dubinskog profiliranja pokazale su da je homogena struktura TiO_2 rutila, invarijantna na varijaciju oksidacijske kinetike. Krivulje *MBI* refleksije fitovane na osnovu Browell-Anderson modela za semitransparentne filmove, pokazale su amplitudnu konvergenciju i faznu divergenciju s rastućom debljinom filma. Dobivena su amplitudna fitovanja bolja od 85% i fazna fitovanja bolja od 95%. Određen je koeficijent ekstinkcije TiO_2, $\beta = 3{,}6 \cdot 10^4\ cm^{-1}$, za valnu dužinu He-Ne lasera ($\lambda = 632{,}8$ nm).